

Electrokinetic Characteristics of Bismuth-Containing Materials Based on Porous Glasses

A. S. Kuznetsova^{a, b, *}, L. E. Ermakova^a, I. N. Anfimova^b, and T. V. Antropova^b

^a*St. Petersburg State University, St. Petersburg, 199034 Russia*

^b*Grebenshchikov Institute of Silicate Chemistry, Russian Academy of Sciences, St. Petersburg, 199034 Russia*

**e-mail: a_kuznetsova95@mail.ru*

Received December 23, 2019; revised January 17, 2020; accepted February 5, 2020

Abstract—Bismuth-containing composite materials based on high-silica porous glasses (PGs) of various types are prepared. Their structural parameters and electrokinetic potential in 10^{-2} M KNO_3 solutions in the pH range 1.5–8.5 are studied. The results are compared with the analogous properties of matrices not modified with bismuth oxide, as well as the pH dependence of the zeta-potential for SiO_2 particles and the sols of synthesized and industrial bismuth(III) oxide. It is determined that modification of larger-pore particles not containing secondary silica with bismuth(III) oxide results in the deviation of the form of the ζ -pH dependences from those intrinsic for high-silica PG and SiO_2 particles.

Keywords: bismuth-containing materials, porous glass, quartz-like glass, electrokinetic potential

DOI: 10.1134/S1087659620030086

INTRODUCTION

High-silica nanoporous glasses are the products of through chemical etching of two-phase alkali-borosilicate glasses; they have comprehensively investigated and are finding an increasing number fields of application [1, 2]. Due to the presence of controlled structural parameters of nanosized pores and high surface reactivity, thermal and chemical stability, relatively low cost, and other characteristics, vitreous materials with the developed pore structure are extensively used as matrices for the preparation of nanostructured composition materials with various functional characteristics caused by the characteristics of the incorporated dopant. Methods for the preparation of such composites based on porous glasses (PGs) modified with alumina and titania [3], gallium nanoparticles [4], haematite ($\alpha\text{-Fe}_2\text{O}_3$) [5], tin and zinc oxides and sulfides [6–8], silver halides [9, 10], and various ferroelectrics [11–13], including PG containing magnetite (Fe_3O_4) [14, 15], are known.

The use of PGs for the preparation of new bismuth-containing composition materials (BCMs) possessing luminescence in the broad spectral range from the visible to the IR range is of particular interest, which makes them promising for use in fiber-optic technologies [16, 17]. Impregnation of PG matrices with bismuth nitrate $\text{Bi}(\text{NO}_3)_3$ from an aqueous salt solution with the subsequent special heat treatment of the impregnated matrices for the formation of bismuth active centers (BACs) is fundamental for the prepara-

tion of such materials [18]. The advantage of this approach lies in the fact that PG is a promising medium, in which the chemical equilibrium of luminescence centers in nanostructures can be effectively controlled.

Information on the relationship of the structure and functional characteristics of the synthesized composites with the structure and colloidal-chemical state of the surface of basic silicate nanoporous matrices is necessary for the targeted synthesis of BCMs with controlled BACs. There are no published data on such studies. In this work, new BCM samples were synthesized according to the procedure in [18] and the structural and electrokinetic characteristics of bismuth-containing porous glass (BPG) and bismuth-containing quartz-like glass (BQG) (sintered up to the collapse of the pores) were studied in aqueous solutions of 0.1 M HNO_3 and 10^{-2} M KNO_3 at various pH values. The characteristics of BCMs were compared with the structural parameters and the values of the electrokinetic potential of PGs not modified with bismuth oxide.

The aim of this work is to prepare nanostructured BCMs and compare the colloidal-chemical characteristics of the parallel PG samples modified and not modified with bismuth(III) oxide.

EXPERIMENTAL

To prepare PG, an 8V-NT sodium-borosilicate glass with a two-framework structure with the composition of $6.74\text{Na}_2\text{O} \cdot 20.52\text{B}_2\text{O}_3 \cdot 72.59\text{SiO}_2 \cdot 0.15\text{Al}_2\text{O}_3$ (wt %) was chosen [19]. In order to form a two-framework structure, the glass was isothermally exposed at 550°C for 144 h. The density of the two-phase glass determined by hydrostatic weighing in water at 20°C corresponded to 2.26 g/cm^3 .

To prepare PGs, the samples of two-phase 8V-NT glass in the form of discs that are 30 mm in diameter and 1 mm in thickness were bleached in 3 M HCl or HNO_3 in a reflux for 3 h. After the treatment of 8V-NT two-phase glass in acid solution, the microporous (MIP) samples (according to the definition of S.P. Zhdanov [20]) were washed in distilled water at room temperature for 5 days and dried at 120°C for 1 h. After that, part of the MIP glass was treated with a 0.5 M solution of KOH at 20°C for 4 h with subsequent washing in distilled water at room temperature and drying in a drying furnace at 120°C . As a result, macroporous (MAP) glass (according to the definition of S.P. Zhdanov [20]) was obtained.

Firstly, the structural parameters (total porosity, structural resistance coefficient, and the tortuosity coefficient) of the PG of various types were determined. Then, a fraction of PG matrices were impregnated in a 0.5 M solution of $\text{Bi}(\text{NO}_3)_3$ prepared based on a 2 M solution of HNO_3 ; and the other part of the matrices, in a 2 M solution of HNO_3 for 1 or 3 days (single- or three-stage treatment) with intermediate drying at 50°C . After impregnation with electrolyte solutions, the samples were exposed to heat treatment with the fulfillment of the temperature–time mode [18] up to the temperature of $T = 650^\circ\text{C}$, as a result of which bismuth nitrate decomposed into bismuth(III) oxide in the pore space of the PGs containing bismuth nitrate (BPG). After repeated measurement of the structural characteristics on heat-treated porous samples, either basic or modified with bismuth oxide, the samples were additionally heat-treated at $T = 870^\circ\text{C}$ until the pores closed with the retention of the formed nanostructures in the case of bismuth-containing glass. The samples of quartz-like glass (QG) and bismuth-containing quartz-like glass (BQG) were obtained.

The surface morphology of the PG was studied using scanning electron microscopy (SEM) on a Zeiss Merlin instrument.

The total porosity of the PG (W) was determined by the gravimetric method. For this purpose, the PG sample was dried to a constant weight at 120°C and weighed in dry form. Then, the disc was maintained for 1 day in bidistilled water with the specific electroconductivity of $1.5 \times 10^{-6}\ \Omega^{-1}\text{ cm}^{-1}$ and weighed at

least five times to determine the mean weight of the water-saturated sample. The value of W was calculated using following equation:

$$W = \frac{(P_m - P_{\text{dry}})}{(P_m - P_{\text{dry}}) + (P_{\text{dry}}\rho_{\text{H}_2\text{O}}/\rho_g)}, \quad (1)$$

where P_m and P_{dry} are the mass of the water-saturated and dry PG, respectively; $\rho_{\text{H}_2\text{O}}$ is the density of water; and ρ_g is the density of the silica matrix of the glass.

The mass of dry and water-saturated samples was determined on a Mettler Toledo Al 204 balance. The measurement error of W was less than $\pm 2\%$.

After the measurements of the bulk porosity, the samples reached equilibrium with a 0.1 M solution of HNO_3 and the specific electroconductivity of the membranes κ_M was measured through the differential method at 20°C (the temperature was set and maintained constant using a LOIPLT-111 thermostat) using an E7-21 immittance meter on alternating current with the frequency of 1000 Hz. The measurement error of the κ_M values was $\pm(2-3)\%$. Since the contribution of the ions of the electrical double layer (EDL) to the electrical conductivity of the porous liquid of weakly charged membranes, which also include PGs, can be neglected at the concentrations of electrolyte solutions $C \geq 0.1\text{ M}$, the structural resistance coefficients β were determined from κ_M , which reflect the contribution of the nonconducting membrane's matrix to their specific electrical conductivity, using the following equation:

$$\beta = (\kappa_V/\kappa_M)|_{C=0.1\text{M}}, \quad (2)$$

where κ_V is the specific electrical conductivity of the free solution. The measurement error of the β values was less than $\pm(2-5)\%$. The values of β were used to evaluate the tortuosity coefficients of the porous channels K . The tortuosity coefficients of the matrices were calculated within the model of cylindrical pores using the following relationship [21]:

$$K^2 = W\beta. \quad (3)$$

After impregnation of the samples in bismuth(III) nitrate or HNO_3 solutions and heat treatment to $T = 650^\circ\text{C}$, the samples with a single- or three-stage treatment were maintained again for 1 day in a decimolar solution of nitric acid for subsequent determination of the final values of the bulk porosity, specific electrical conductivity of the membranes, the structural resistance coefficient, and the tortuosity coefficient of the pores.

The bismuth content in BPG was studied using X-ray energy dispersive spectroscopy (EDS) (Oxford Instruments INCAx-act spectrometer) and X-ray fluorescent analysis (XRF) (Shimadzu EDX-800P energy dispersive X-ray fluorescence spectrometer).

Table 1. Composition and structural parameters of PG

PG	Content according to analysis, wt %					Porosity W , cm ³ /cm ³ (%)	Apparent density ρ , g/cm ³	Specific pore surface S_{sp} , m ² /g	Mean pore diameter D , nm
	SiO ₂	Na ₂ O	K ₂ O	B ₂ O ₃	Al ₂ O ₃				
MIP	97.11	0.42	0.07 (traces)	2.29	0.11	0.29 (29)	1.6692	164	3
MAP	94.51	0.66	0.50	4.21	0.12	0.59 (59)	1.0140	73	25

Using the EDS method, the thickness distribution of bismuth in the MAP membrane impregnated in a bismuth nitrate solution for 72 h (three-stage treatment) was also studied.

To study the electrokinetic characteristics, the PG samples both modified and not modified with bismuth oxide and sintered until the pores closed at $T = 870^\circ\text{C}$ were used. The QG and BQG samples were ground in agate mortar and the glass shots (0.01 g) were transferred to the flasks filled with 40 mL of a 10^{-2} M solution of KNO_3 . The specific pH value in the suspensions was achieved using 2 or 0.1 M HNO_3 and 0.01 M KOH. The electrophoretic mobility (U_e) of the QG and BQG particles was measured using laser Doppler electrophoresis (ZetasizerNano ZS, Malvern). Several series of measurements were carried out at each concentration of the background electrolyte and the results were averaged. In order to evaluate the conversion of the modification of the PG matrices with bismuth oxide, the electrokinetic potential of the synthesized and industrial bismuth oxide was measured in a 10^{-2} M solution of KNO_3 . The synthesized bismuth oxide was prepared as a result of the thermal decomposition of a 0.5 M solution of $\text{Bi}(\text{NO}_3)_3$ based on the 2 M solution of HNO_3 through heating to $T = 650^\circ\text{C}$ in a muffle furnace in accordance with the heat treatment mode of the PG impregnated with a bismuth nitrate solution. It should be noted that the same monoclinic modification of bismuth oxide was detected in both samples according to the X-ray phase analysis (PCPDFwin, 76-1730).

To prepare Bi_2O_3 sols, shots (2 g) of the synthesized and industrial bismuth oxide preliminarily ground in agate mortar were transferred to glass beakers and a total of 200 mL of deionized water was added followed by the transfer of the beakers to a UZV-7/100-TNM ultrasound bath) for 4 and 5 h with the modulation frequency of 150 Hz. A total of 20 mL of sol and 20 mL of the 2×10^{-2} M solution of KNO_3 were selected in flasks for study and HNO_3 or KOH were added to give the specified pH value of the suspension.

The pH of the solutions were measured using a Seven S-80KMettler Toledo pH meter. The electrolyte solutions were prepared using the standard solutions and the reagents of extra-pure grade using deionized water (a UVOI-M-F water purification setup, $\kappa_v \leq 1.5 \times 10^{-6} \Omega^{-1} \text{cm}^{-1}$).

RESULTS AND DISCUSSION

Table 1 shows the data on the chemical composition and structural parameters of the pore space of the PGs [19, 22, 23].

Figures 1a–1c show the SEM images of the front surface of the initial PG matrix from the MAP glass, taken from the cleavage of the BQG from the MAP glass after three-stage impregnation with a nitric-acid solution of bismuth nitrate with the subsequent heat treatment at 650°C , and the front surface of the BQG from the MAP glass ($T = 870^\circ\text{C}$) after a single-stage treatment, respectively. It is clear that the heat treatment of PG at 870°C results in the pores almost completely closing.

The results of measuring and calculating the W , β , and K values of the PG before and after impregnation with electrolyte solutions are given in Table 2. The results of the calculation of the β and K coefficients show that maintenance of the MIP and MAP matrices for 1 or 3 days in highly concentrated electrolyte solutions and subsequent heat treatment at 650°C results in a significant decrease in the β values (by $\sim 24\%$) and a marginal change of the K values for the MIP glass, while these parameters for the MAP glass barely change. The observed principles can be related to the structural change of secondary silica in the pore space of the MIP glass and its almost complete absence in the MAP glass. The presence of Bi_2O_3 in the pore space of the matrices does not alter the change in the β and K values as a result of the heat treatment.

The results of the bulk porosity measurements of the PG show that impregnation with an electrolyte solution and thermal treatment of the PG at 650°C result in the marginal growth of the W values for all the samples except for the MAP glass with a three-stage treatment with a bismuth nitrate solution. The observed changes can be related to the structural thickening of the secondary silica in the space of the MIP glass and to the formation of bismuth oxide aggregates in the pore space of the MAP glass.

Table 3 shows the relative bismuth content in the MIP and MAP glass modified with bismuth(III) oxide according to the EDS and XRF data. It is clear that an increase in the impregnation time from 24 to 74 h results in the increase in the relative bismuth content in the micro- and macroporous glasses, which agrees with the data from [16] obtained during impregnation

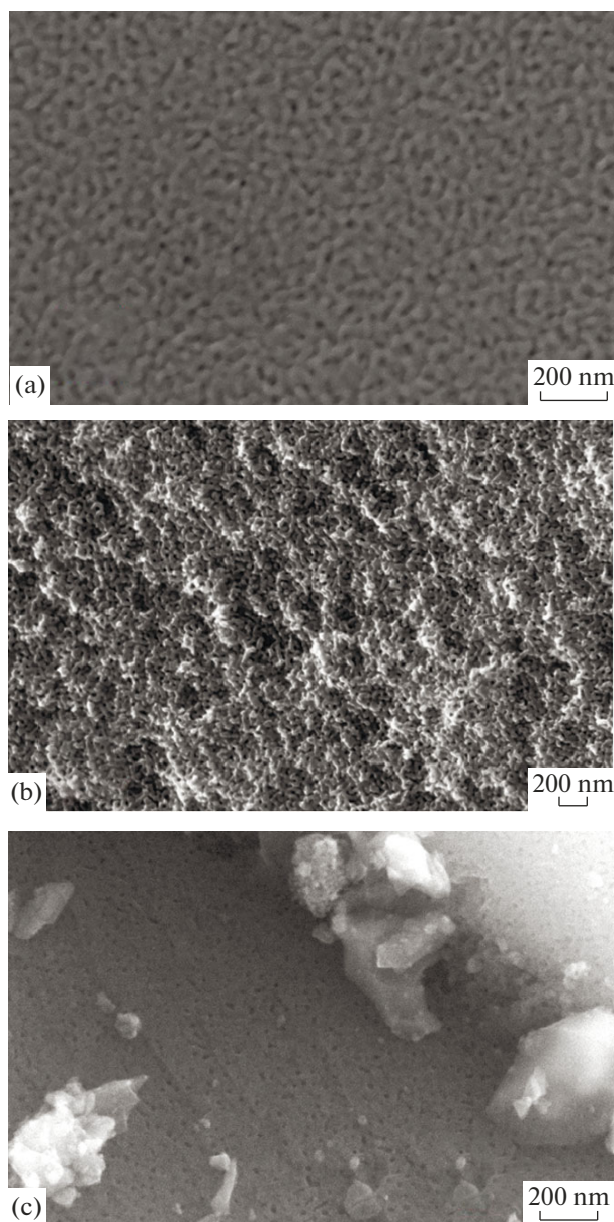


Fig. 1. SEM images of the (a) surface of MAP glass without impregnation [24], (b) taken from the cleavage of the bismuth-containing MAP glass with three-stage impregnation and heat treatment at $T = 650^\circ\text{C}$, and (c) the surface of bismuth-containing quartz-like glass based on MAP glass with single-stage impregnation.

of the PG matrices in the form of thicker plates. Figure 2 demonstrates the thickness distribution of bismuth in the the BQG MAP samples with a three-stage impregnation and heat treatment at 650°C . The bismuth is mainly located at the half-thickness of the sample in contrast to the thicker samples in the form of plates [25].

The electrokinetic potential (ζ^S) can be calculated from the electrophoretic mobility U_e determined by

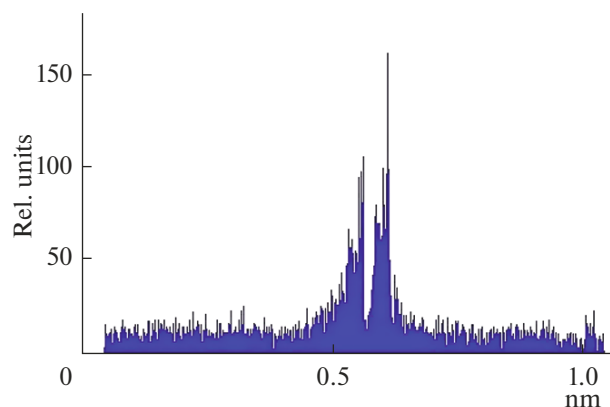


Fig. 2. EDX image of bismuth thickness distribution in bismuth-containing MAP glass with three-stage impregnation and heat treatment at $T = 650^\circ\text{C}$.

laser Doppler electrophoresis according to the Helmholtz–Smolukhovskii equation

$$\zeta^S = \frac{\eta}{\varepsilon\varepsilon_0} U_e, \quad (4)$$

where η is the viscosity of the medium and ε and ε_0 are the dielectric permittivity of the medium and vacuum, respectively.

Figure 3a shows the dependences of the electrophoretic mobility and zeta potential of the QG and BQG particles based on the MIP glass and monodisperse ($0.56 \mu\text{m}$) SiO_2 particles on the pH in the background of a 10^{-2}M solution of KNO_3 [26]. It is clear that the values of the U_e and ζ^S potential of the BQG prepared through single-stage or three-stage impregnation of the MIP glass in $\text{Bi}(\text{NO}_3)_3$ solutions coincide with the values of the QG kept in HNO_3 solutions. Thus, the presence of 0.5 to 1.0 wt % of bismuth in the PG matrices barely affects their electrokinetic characteristics. A comparison of the electrokinetic potential of the QG and BQG with the ζ^S potential of monodisperse silica particles (curve *b*) showed that the absolute values of the ζ^S potential of SiO_2 particles at $\text{pH} < 5$ are less than those in the case of the particles of quartz-like glass of various compositions. The isoelectric point (IEP) of SiO_2 is observed at a pH of 2.85, while a positive region of the ζ^S potential was not found in the case of quartz-like glass in the studied pH range. At a pH of 5 to 6, the electrokinetic potentials of the quartz-like glass particles and silica particles are similar.

The dependences of the electrokinetic characteristics of the QG and BQG particles prepared based on the MAP glass possessing a higher degree of porosity (Table 1) on the pH in the background of a 10^{-2}M solution of KNO_3 are given in Fig. 3b. In the case of the sintered MAP glass modified with bismuth(III)

Table 2. Structural parameters of initial matrices (nos. 1 and 2 in each type of PG) and the same matrices after impregnation with solutions and heat treatment

No., treatment	d_M , cm	β	W	K
Single-stage impregnation with electrolyte and heat treatment				
8V-NT MIP (3 M HCl)*				
1	0.1007	28.78	0.233	2.59
1 + Bi(NO ₃) ₃ + 650°C	0.1007	19.57	0.241	2.17
2	0.0965	28.22	0.239	2.60
2 + HNO ₃ + 650°C	0.0965	20.94	0.250	2.29
8V-NT MIP (3 M HNO ₃)				
1	0.0996	31.20	0.236	2.71
1 + Bi(NO ₃) ₃ + 650°C	0.0996	22.41	0.242	2.33
2	0.0971	31.00	0.230	2.67
2 + HNO ₃ + 650°C	0.0971	23.80	0.245	2.42
8V-NT MAP (3 M HNO ₃ + 0.5 M KOH)				
1	0.1013	2.68	0.585	1.25
1 + Bi(NO ₃) ₃ + 650°C	0.1013	2.64	0.591	1.25
2	0.0980	2.76	0.586	1.27
2 + HNO ₃ + 650°C	0.0980	2.90	0.593	1.31
Three-stage impregnation with electrolyte and heat treatment				
8V-NT MIP (3 M HCl)				
1	0.091	27.78	0.243	2.60
1 + Bi(NO ₃) ₃ + 650°C	0.091	22.12	0.242	2.31
2	0.100	24.42	0.244	2.44
2 + HNO ₃ + 650°C	0.100	22.44	0.245	2.34
8V-NT MIP (3 M HNO ₃)				
1	0.0995	30.46	0.239	2.70
1 + Bi(NO ₃) ₃ + 650°C	0.0995	23.74	0.244	2.41
2	0.0995	29.61	0.237	2.65
2 + HNO ₃ + 650°C	0.0995	23.67	0.247	2.42
8V-NT MAP (3 M HNO ₃ + 0.5 M KOH)				
1	0.097	2.82	0.548	1.24
1 + Bi(NO ₃) ₃ + 650°C	0.097	2.96	0.518	1.24

*Labeling of membranes corresponds to the fabrication conditions of PG.

oxide, there is a deviation of the ζ^S -pH dependence from the typical dependence in the case of high-silica PG matrices. The electrokinetic potential of BQG with single-stage impregnation increases by absolute value at the pH of 1.2 to 3 and, then, it decreases to 5.5 mV; starting from pH 4, the ζ^S potential increases again. With an increase in the time of impregnation of the MAP matrices with bismuth nitrate solutions from 24 to 72 h and, accordingly, with an increase in the relative bismuth content from 2.5 to 3.1 wt %, the appear-

ance of a positive range of the electrokinetic potential is observed at a pH of 2.3 to 6.7.

It is natural to suggest that the presence of bismuth in the PG matrix would affect the form of the ζ^S -pH dependence. In this case, the difference of the form of the ζ^S -pH dependences of the BQG samples, which were obtained from the MIP and MAP glass (Figs. 3a, 3b), can be related to the different bismuth content (Table 3). Figure 4 shows the dependence of the electrophoretic mobility and zeta potential of the synthesized and

Table 3. Relative bismuth content in PGs

Bismuth content	Membranes					
	MIP (3 M HCl), 1 stage	MIP (3 M HNO ₃), 1 stage	MAP, 1 stage	MIP (3 M HCl), 3 stages	MIP (3 M HNO ₃), 3 stages	MAP, 3 stages
Atomic %	—	0.06	0.28	0.05*	0.11	0.35*
Weight %	—	0.56	2.54	0.41*	1.01	3.14*

*Using XRF method.

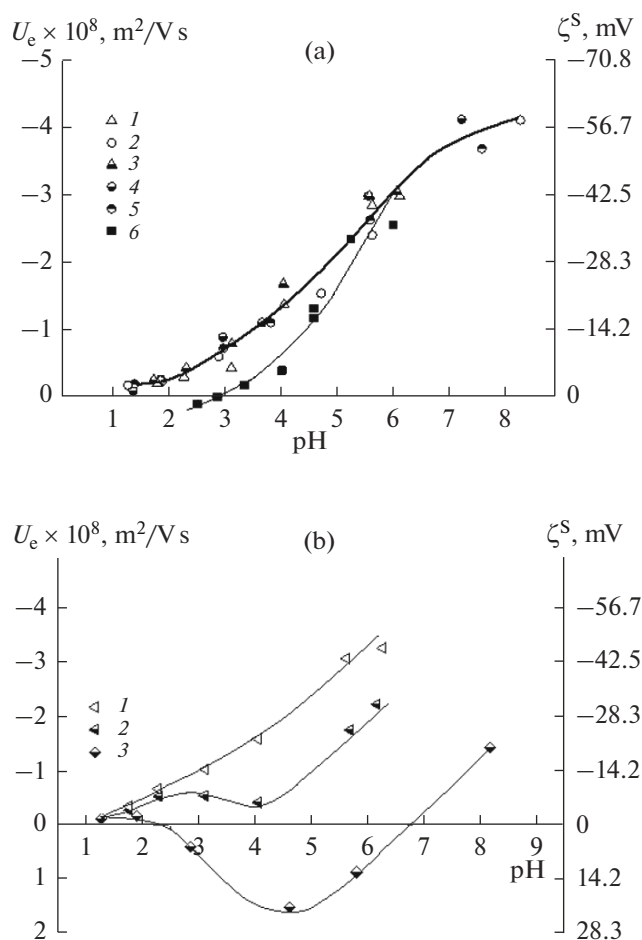


Fig. 3. Dependence of electrophoretic mobility and zeta potential of QG and BQG obtained from (a) MIP or (b) MAP glass on pH in the background of 10^{-2} M solution of KNO_3 . (a) (1) QG from MIP (3 M HNO_3), single-stage impregnation in 2 M solution of HNO_3 , (2) QG from MIP (3 M HNO_3), three-stage impregnation in 2 M solution of HNO_3 , (3) BQG from MIP (3M HNO_3), single-stage impregnation in 0.5 M solution of bismuth nitrate, (4) BQG from MIP (3 M HNO_3), three-stage impregnation in 0.5 M solution of bismuth nitrate, (5) BQG from MIP (3 M HCl), three-stage impregnation in 0.5 M solution of bismuth nitrate, (6) monodisperse SiO_2 particles with the radius of $0.56 \mu\text{m}$ [26]; (b) (1) QG from MAP, single-stage impregnation in 2 M solution of HNO_3 , (2) BQG from MAP, single-stage impregnation in in 0.5 M solution of bismuth nitrate, (3) BQG from MAP; three-stage impregnation in 0.5 M solution of bismuth nitrate.

industrial bismuth oxide on pH on the background of a 10^{-2} M solution of KNO_3 . The values of the electrokinetic characteristics in both cases are similar and positive in the entire pH range. The observed form of the U_e -pH dependence indicates that the IEP of the bismuth oxide samples is in the alkaline pH range (at $\text{pH} > 9.5$). The drastic decrease in the U_e and ζ^S potential at $\text{pH} < 3$ is presumably caused by the increase in the ionic strength of the solution, which results in a decrease in the zeta potential due to the compressing of the diffuse part of the EDL. As follows from Fig. 4, the electrokinetic potential of bismuth(III) oxide varies from 41 to 30 mV at a pH of 2.3 to 6.7, in which there is a positive electrokinetic potential of the BQG (Fig. 3b). At a pH of 6.7 to 8, corresponding to a decrease in the positive value of the electrokinetic potential of bismuth oxide from 30 to 21 (Fig. 4), the values of the ζ^S potential of the BQG (Fig. 3b) pass the second isoelectric point and become negative again at $\text{pH} > 6.7$. In the case of the BQG based on the MIP glass (Fig. 3a), the bismuth content is low (compared to the MAP glass) and does not significantly affect the form of the ζ^S -pH dependence.

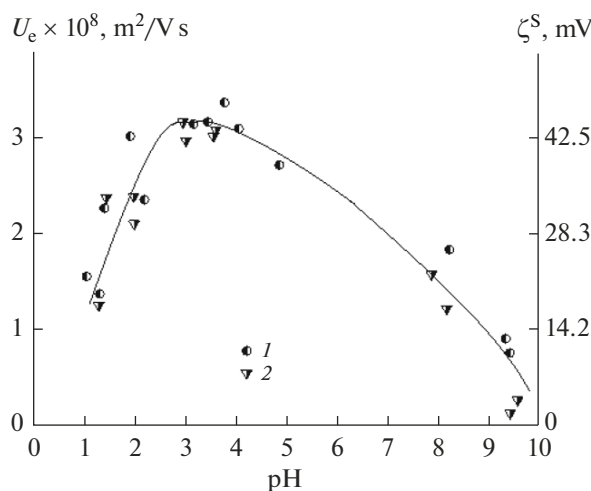


Fig. 4. Dependence of electrophoretic mobility and zeta potential of (1) synthesized and (2) industrial bismuth oxide on pH in the background of 10^{-2} M solution of KNO_3 .

CONCLUSIONS

The high-silica PG of two types and bismuth-containing vitreous composite materials based on them have been obtained. The structural characteristics and electrokinetic potential of the glass with different compositions have been studied and compared on the background of a centimolar solution of potassium nitrate in a broad pH range. It has been shown that the relative bismuth content in a composite increases with an increase in the pore size and porosity of the PG samples and with an increase in the time of their impregnation with a 0.5 M solution of bismuth nitrate. The modification of MIP glass with bismuth oxide (the bismuth oxide content is less than 0.5 wt %) does not affect its electrokinetic characteristics in contrast to the BQG prepared using MAP glass. An increase in the impregnation time of MAP glass with a bismuth nitrate solution from 24 to 72 h and, accordingly, an increase in the bismuth oxide content in the nanocomposite up to 2.5–3 wt % results in the appearance of a positive region of the electrokinetic potential of the BQG particles. The values of the electrokinetic potential of industrial bismuth oxide and Bi₂O₃ prepared through the thermolysis of bismuth nitrate under laboratory conditions in the background of a centimolar solution of potassium nitrate are similar to each other and are positive in the entire pH range.

ACKNOWLEDGMENTS

The authors thank M.A. Girsova for her help in the thermal treatment of the composites and I.G. Polyakova for the X-ray phase analysis of bismuth oxides. The studies were carried out using the equipment of the Resource Centers of the Research Park of St. Petersburg State University “Nanotechnologies” and “Methods of analysis of the composition of a substance.”

FUNDING

The work was supported by the Russian Foundation for Basic Research (project no. 18-03-01206). The samples of two-phase glass and PG were fabricated as part of a state task (0097-2019-0015) of the Grebenshchikov Institute of Silicate Chemistry of the Russian Academy of Sciences.

CONFLICT OF INTEREST

The authors declare that they have no conflict of interest.

REFERENCES

1. Antropova, T.V., Inorganic functional glass-forming materials based on liquating alkaline borosilicate systems, in *IKhS RAN-80 let. Sovremennye problemy neorganicheskoi khimii* (Inst. Silicate Chem. RAS 80th Anniversary, Modern Problems of Inorganic Chemistry), Shevchenko, V.Ya., Ed., St. Petersburg: Art.-Ekspress, 2016, pp. 117–137.
2. Inayat, A., Reinhardt, B., Herwig, J., Küster, C., Uhlig, H., Krenkel, S., Raedlein, E., and Enke, D., Recent advances in the synthesis of hierarchically porous silica materials on the basis of porous glasses, *New J. Chem.*, 2016, vol. 40, no. 5, pp. 4095–4114.
3. Ermakova, L.E., Volkova, A.V., Antropova, T.V., Orbelli, N.O., and Anfimova, I.N., Electrokinetic characteristics of initial porous glasses and those modified with titanium- and aluminum-oxide particles, *Colloid J.*, 2017, no. 6, pp. 762–772.
4. Chamaya, E.V., Tien, C., Wur, C.S., and Kumzerov, Yu.A., Superconductivity of gallium in porous glass, *J. Phys. C: Solid State Phys.*, 1996, vol. 269, pp. 313–324.
5. Golosovsky, I.V., Mirebeau, I., Fauthc, F., Kurdyukov, D.A., and Kumzerov, Yu.A., Magnetic structure of hematite nanostructured in a porous glass, *Solid State Commun.*, 2007, vol. 141, pp. 178–182.
6. Yang, K., Zheng, Sh., Jiang, X., Fan, Sh., and Chen, D.-P., Luminescence and scintillation of high silica glass containing SnO, *Mater. Lett.*, 2017, vol. 204, pp. 5–7.
7. Sidorov, A.I., Ngo Dui Tung, Ngo Van Wu, Antropova, T.V., and Nashchekin, A.V., Optical properties of nanocomposites based on zinc and tin sulfides in nanoporous silicate glass, *Opt. Spectrosc.*, 2019, vol. 127, no. 5, pp. 914–918.
8. Sidorov, A.I., Ngo Dui Tung, Ngo, Van Wu, N., Antropova, T.V., Nashchekin, A.V., Castro, R., and Anfimova, I.I., Optical and dielectric properties of nanocomposites based on zinc and tin oxides in nanoporous glass, *Glass Phys. Chem.*, 2019, vol. 45, no. 6, pp. 421–428.
9. Antropova, T., Girsova, M., Anfimova, I., Drozdova, I., Polyakova, I., and Vedishcheva, N., Structure and spectral properties of the photochromic quartz-like glasses activated by silver halides, *J. Non-Cryst. Solids*, 2014, vol. 401, pp. 139–141.
10. Antropova, T.V., Girsova, M.A., Anfimova, I.N., and Drozdova, I.A., Spectral properties of the high-silica porous glasses doped by silver halides, *J. Lumin.*, 2018, vol. 193, pp. 29–33.
11. Cizman, A., Antropova, T., Anfimova, I., Drozdova, I., Rysiakiewicz-Pasek, E., Radoewska, E.B., and Poprawski, R., Size-driven ferroelectric-paraelectric phase transition in TGS nanocomposites, *J. Nanopart. Res.*, 2013, vol. 15, no. 8, 1807. <https://doi.org/10.1007/s11051-013-1807-y>
12. Cizman, A., Marcinişzyn, T., Rysiakiewicz-Pasek, E., Sieradzki, A., Antropova, T.V., and Poprawski, R., Size effects in KDP-porous glass ferroelectric nanocomposites, *Phase Trans.*, 2013, vol. 86, no. 9, pp. 910–916.
13. Rysiakiewicz-Pasek, E., Cizman, A., Drozdova, I., Polyakova, I., and Antropova, T., Synthesis, structure and properties of mixed KNO₃–NaNO₃ embedded into nanoporous silica glass, *Composites, Part B*, 2016, vol. 91, pp. 291–295.
14. Cizman, A., Rogacki, K., Rysiakiewicz-Pasek, E., Antropova, T., Pshenko, O., and Poprawski, R., Magnetic properties of novel magnetic porous glass-based multi-

- ferroic nanocomposites, *J. Alloys Compd.*, 2015, vol. 649, pp. 447–452.
15. Ermakova, L.E., Kuznetsova, A.S., Volkova, A.V., and Antropova, T.V., Structural and electro-surface properties of iron-containing nanoporous glasses in KNO_3 solutions, *Colloids Surf., A*, 2019, vol. 576, pp. 91–102.
 16. Girsova, M.A., Firstov, S.V., and Antropova, T.V., The influence of the bismuth concentration and heat treatment on the properties of bismuth-containing high-silica glass. II. Luminescence properties, *Glass Phys. Chem.*, 2019, vol. 45, no. 2, pp. 98–103.
 17. Dianov, E.M., Yang, L., Iskhakova, L.D., Vel'miskin, V.V., Plastinin, E.A., Milovich, F.O., Mashinskii, V.M., and Firstov, S.V., Use of nanoporous glass for the fabrication of heavily bismuth-doped active optical fibres, *Quantum Electron.*, 2018, vol. 48, no. 7, pp. 658–661.
 18. Antropova, T.V., Girsova, M.A., Anfimova, I.N., Golovina, G.F., Kurilenko, L.N., and Firstov, S.V., RF Patent 2605711, *Byull. Izobret.*, 2016, no. 34.
 19. Antropova, T.V., Girsova, M.A., Anfimova, I.N., and Drozdova, I.A., Spectral properties of the high-silica porous glasses doped by silver halides, *J. Lumin.*, 2018, vol. 193, pp. 29–33.
 20. Zhdanov, S.P., Porous glasses and their structure, *Wiss. Z. Friedrich-Schiller-Univ., Jena: Naturwiss. Reihe*, 1987, vol. 36, pp. 817–830.
 21. Ermakova, L.E., Antropova, T.V., Volkova, A.V., Kuznetsova, A.S., Grinkevich, E.A., and Anfimova, I.N., Structural parameters of membranes from porous glass in aqueous solutions of electrolytes, containing singly-charged (Na^+ , K^+) and triple-charged (Fe^{3+}) cations, *Glass Phys. Chem.*, 2018, vol. 44, no. 4, pp. 269–278.
 22. Antropova, T., Girsova, M., Anfimova, I., Drozdova, I., Polyakova, I., and Vedishcheva, N., Structure and spectral properties of the photochromic quartz-like glasses activated by silver halides, *J. Non-Cryst. Solids*, 2014, vol. 401, pp. 139–141.
 23. Kreisberg, V.A. and Antropova, T.V., Changing the relation between micro- and mesoporosity in porous glasses: The effect of different factors, *Microporous Mesoporous Mater.*, 2014, vol. 190, no. 1, pp. 128–138.
 24. Kuznetsova, A.S., Volkova, A.V., Ermakova, L.E., and Antropova, T.V., Iron(III) ion adsorption on macroporous glass, *Glass Phys. Chem.*, 2018, vol. 44, no. 1, pp. 41–46.
 25. Girsova, M.A., Golovina, G.F., Anfimova, I.N., and Kurilenko, L.N., Properties of bismuth-containing high-silica glass depending on the bismuth concentration and heat treatment. I. Spectral-optical properties, *Glass Phys. Chem.*, 2018, vol. 44, no. 5, pp. 381–387.
 26. Sidorova, M.P., Zastrow, H., Ermakova, L.E., Bogdanova, N.F., and Smirnov, V.M., Synthesis of titanium–oxygen layers on silicon oxide monodisperse particles and comparison between the electro-surface characteristics of the initial and modified particles, *Colloid J.*, 1999, vol. 61, pp. 104–109.

Translated by A. Muravev